Endonuclease III Is an Iron–Sulfur Protein†

Richard P. Cunningham,* Hitomi Asahara, and Janet F. Bank
Department of Biological Sciences, Center for Biochemistry and Biophysics, State University of New York at Albany, Albany, New York 12222

Charles P. Scholes
Department of Physics, Center for Biochemistry and Biophysics, State University of New York at Albany, Albany, New York 12222

John C. Salerno
Department of Biology, Center for Biophysics, Rensselaer Polytechnic Institute, Troy, New York 12180

Kristene Surerus and Eckard Münck
Gray Freshwater Biological Institute, University of Minnesota, Navarre, Minnesota 55392

John McCracken and Jack Peisach
Biotechnology Resource in Pulsed EPR Spectroscopy, Albert Einstein College of Medicine, 1300 Morris Park Avenue, Bronx, New York 10461

Mark H. Emptage
Central Research and Development Department, Experimental Station, E. I. du Pont de Nemours and Company, Wilmington, Delaware 19880-0328

Received November 28, 1988; Revised Manuscript Received January 31, 1989

ABSTRACT: Elemental analyses, Mössbauer, and EPR data are reported to show that endonuclease III of *Escherichia coli* is an iron–sulfur protein. Mössbauer spectra of protein freshly prepared from *E. coli* grown on ^{57}Fe-enriched medium demonstrate that the native enzyme contains a single 4Fe–4S cluster in the 2+ oxidation state, with a net spin of zero. Upon treatment with ferricyanide, a fraction (<25%) of the clusters is oxidized into a state which yields an EPR spectrum near $g = 2.01$ typical of a 3Fe–4S cluster. The magnetic field dependence of the linear electric field effect verifies this assignment. Electron spin echo modulation on the $g = 2.01$ form of the protein in deuterated solvent indicates the presence of exchangeable protons in the vicinity of the 3Fe–4S cluster. The data obtained show that the $[4Fe–4S]^{2+}$ cluster of the native enzyme is resistant to either oxidation or reduction, although photoreduction elicited a $g = 1.94$ type EPR signal characteristic of a $[4Fe–4S]^{1+}$ cluster. These studies show that endonuclease III is unique in being both a DNA repair enzyme and an iron–sulfur protein. The function of the 4Fe–4S cluster remains to be established.

In general, iron–sulfur proteins containing 4Fe–4S clusters are utilized for electron transport. However, it has been shown in recent years that these clusters may also function as substrate binding sites in catalytic reactions (Beinert & Thomson, 1983; Emptage, 1988). It has been shown by Mössbauer spectroscopy (Kent et al., 1982) that substrate and inhibitors bind to one of the iron atoms (site A) of the $[4Fe–4S]^{2+}$ cluster of beef heart aconitase. In vivo, the active form of the cluster is most likely the diamagnetic 2+ core oxidation state. By reducing the aconitase cluster, one attains a state which can be probed with electron paramagnetic resonance (EPR)[1] and ENDOR as well as by Mössbauer spectroscopy (Kent et al., 1985). ENDOR studies of reduced aconitase with isotopically enriched substrates have shown that its active 4Fe–4S center is part of a catalytic site that interconverts citrate, *cis*-aconitate, and isocitrate (Telser et al., 1986; Kennedy et al., 1987). Exposure of aconitase to air causes the loss of the iron of site A from the cluster, resulting in a structure with a $[3Fe–4S]^{1+}$ core (Kent et al., 1982). Such clusters yield, in the oxidized state, an EPR signal near $g = 2.01$. Similar signals are obtained when certain 4Fe–4S clusters are treated with ferricyanide (Beinert & Thomson, 1983).

Until 1980, it was thought that one could identify 2Fe–2S and 4Fe–4S clusters by core extrusion techniques (Beinert & Thomson, 1983; Kurtz et al., 1979). However, when such methods were applied directly to aerobically purified aconitase (which contains a 3Fe–4S cluster), it became clear that this technique was unreliable and that spectroscopic techniques had to be used for unambiguous cluster identification (Beinert et al., 1983; Peisach et al., 1983).

The bacterial protein glutamine phosphoribosylpyrophosphate amidotransferase from *Bacillus subtilis* contains a diamagnetic $[4Fe–4S]^{2+}$ center whose integrity is essential for enzymatic function (Averill et al., 1980). The exact role of this 4Fe–4S center in the catalytic mechanism is not yet obvious (Vollmer et al., 1983). The enzyme is very stable in the absence of oxygen and active in its diamagnetic $[4Fe–4S]^{2+}$ state (Averill et al., 1980). Unlike aconitase, only a small

† This research was supported by U.S. Public Health Service Grants GM-33346 (R.P.C.), GM-34306 (J.C.S.), GM-35103 (C.P.S.), and RR02583 (J.P.) and by National Science Foundation Grant DBM-86050050 (E.M.).

* Author to whom correspondence should be addressed.

[1] Abbreviations: AP, apurinic and/or apyrimidinic; ENDOR, electron nuclear double resonance; EPR, electron paramagnetic resonance; ESEEM, electron spin echo envelope modulation; G, gauss (1 gauss = 10^{-4} tesla); LEFE, linear electric field effect; ptp, peak to peak; T, tesla.

0006-2960/89/0428-4450$01.50/0

fraction of the amidotransferase can be converted to a paramagnetic species with EPR features similar to other 3Fe–4S proteins (Vollmer et al., 1983).

Endonuclease III has been shown to have both *N*-glycosylase activity on DNA that contains damaged bases and AP endonuclease activity (Demple & Linn, 1980; Katcher & Wallace, 1983; Breimer & Lindahl, 1984). The glycosylase activity releases a number of ring-saturated and ring-fragmented derivatives of thymine, including thymine glycol, 5,6-dihydrothymine, urea, 5-hydroxy-5-methylhydantoin, and methyltartronylurea (Demple & Linn, 1980; Breimer & Lindahl, 1980, 1984, 1985; Katcher & Wallace, 1983). In addition, endonuclease III also releases an unidentified cytosine photoproduct (Doetsch et al., 1986; Weiss & Duker, 1986) and incises damaged DNA at cytosines (Doetsch et al., 1986, 1987; Helland et al., 1986; Weiss & Duker, 1986, 1987). The AP endonuclease activity is the result of the enzyme catalyzing a β-elimination reaction at AP sites (Bailly & Verly, 1987; Kow & Wallace, 1987). Recent studies suggest that the *N*-glycosylase and the AP endonuclease activities act in concert, and it was determined that the product thymine glycol inhibits the *N*-glycosylase activity (Kow & Wallace, 1987).

In this paper, we describe the iron–sulfur clusters in native and oxidized endonuclease III. Using a combination of spectroscopic methods together with chemical analysis, we demonstrate that the active protein 4Fe–4S cluster in the divalent oxidation state, upon ferricyanide oxidation, loses an iron atom to form an EPR-active 3Fe cluster.

Materials and Methods

Preparation of Endonuclease III. Endonuclease III was prepared, purified, and assayed according to methods of the preceding paper (Asahara et al., 1989). For Mössbauer samples, the *Escherichia coli* were grown on a minimal medium containing a concentration of 5 μM 95.15% ^{57}Fe (Siegel et al., 1973). The specific activity of this latter, ^{57}Fe-containing enzyme was the same as non-^{57}Fe-enriched enzyme (Asahara et al., 1989). Photoreductions of endonuclease III were done following the procedures of Massey and Hemmerich (1978) using 0.005 mM deazaflavin, 5 mM potassium oxalate, and 1 mM dithiothreitol in 0.1 M potassium phosphate, pH 6.6. Anaerobic samples in glass-stoppered EPR tubes were irradiated with light originating from a 500-W projector lamp using a 12-cm path-length glass container as an IR filter. The extent of reduction was determined by taking optical spectra through the EPR tube on a HP8451A diode array spectrophotometer using a specially constructed black delrin EPR tube holder with a 2-mm light slit.

Fe and S Analysis. Iron analysis was done by the method of Kennedy et al. (1984), and sulfide analysis was done by the method of Fogo and Popowsky (1949) as modified by Beinert (1983). These analyses were also carried out on the Mössbauer sample and subsequent enzyme preparations.

EPR Methods. In uncovering some of the first clues that endonuclease III was an Fe–S protein, EPR spectra were taken for the protein as initially prepared in pH 6.6, 0.1 M phosphate buffer, and next on protein oxidized by potassium ferricyanide. EPR studies of oxidized samples gave results highly reminiscent of previously studied 3Fe–4S proteins (Beinert & Thomson, 1983). A mole ratio of about 3:1 ferricyanide to protein and a 10–30-min reaction time gave the optimum signal.[2] It was found that the EPR signal was occasionally enhanced but resolution of *g*-value details lost if the sample was warmed and refrozen.

Samples for pulsed EPR were concentrated with an Amicon ultrafiltration device to a concentration of about 0.5 mM; the ferricyanide was added before completion of the concentration process so that a 10-fold dilution of ferricyanide with respect to protein took place during the final concentration process. The deuterated samples for pulsed EPR were concentrated vs two changes of deuterated buffer to an approximate 95% exchangeable deuterium enrichment.

Standard EPR measurements as in Figures 2 and 5 were carried out with an IBM-Bruker ER-200 EPR spectrometer fitted with an Air Products Model LTD 3-110 liquid helium flow system and temperature controller. Simulations of the spectrum of Figure 2 were done by the methods of Salerno and Ohnishi (1980) in order to determine the *g* values and concomitant line widths. Also, a simulation of the EPR spectrum from a sample of myoglobin azide was done for comparison purposes in determining the number of spins in the oxidized endonuclease III sample. The number of spins in the photoreduced sample was estimated by comparing the double integral of its EPR signal to that of a Cu^{2+}-EDTA standard.

Electron spin echo experiments were perfomed at pumped helium temperatures using a spectrometer described elsewhere (McCracken et al., 1987). In the LEFE experiments, the two-pulse echo was diminished by an applied electric field, where the electric field (E) and the applied magnetic field (H_0) were oriented either parallel ($E_\parallel H_0$) or perpendicular ($E_\perp H_0$) to each other. LEFE shift parameters, σ, were calculated by the half-fall method, i.e., the electric field required to reduce the spin-echo amplitude to half its unperturbed value (Mims, 1974; Mims & Peisach, 1979), and plotted vs magnetic field, as in Figure 3. Electron spin echo envelope modulation (ESEEM) experiments, both two- and three-pulse, were done to probe for exchangeable protons near the paramagnetic metal center.

The Mössbauer sample was stored in liquid nitrogen. For the measurements, it was transferred into a Janis SuperVaritemp cryostat or into a dewar fitted with a 6.0-T superconducting magnet. The isomer shift, δ, is referred to Fe metal at room temperature.

Results

Elemental Analyses. In preliminary qualitative experiments, release of H_2S upon acidification of the protein made us aware that endonuclease III might be an Fe–S protein. Initial quantitative analyses on a sample which had been stored at −20 °C for three months yielded 2.7 ± 0.2 Fe and 2.1 ± 0.2 labile sulfides per 23.5-kDa monomer. The freshly prepared Mössbauer sample used here yielded 3.9 ± 0.2 Fe per monomer, and that freshly prepared for enzyme studies yielded 3.8 ± 0.2 Fe per monomer.

Mössbauer Results. Figure 1 shows a 4.2 K Mössbauer spectrum of a ^{57}Fe-enriched sample of endonuclease III. The zero-field spectrum shown in Figure 1A consists of a symmetric quadupole doublet with quadrupole splitting, ΔE_Q = 1.18 ± 0.02 mm/s, and isomer shift, δ = 0.44 ± 0.01 mm/s (relative to Fe metal at 300 K). The absorption lines are sharp, with a full width at half-maximum of 0.27 mm/s. ΔE_Q is essentially independent of temperature, and the isomer shift displays the typical second-order Doppler shift as the temperature is increased; at 103 K, we found ΔE_Q = 1.13 ± 0.02 mm/s and δ = 0.42 ± 0.01 mm/s.

Figure 1B shows a 4.2 K spectrum recorded in a parallel field of 6.0 T. The observed spectral pattern is typical of a

[2] Those samples that were allowed to remain oxidized overnight in the presence of ferricyanide were found bleached and smelled of H_2S the next day.

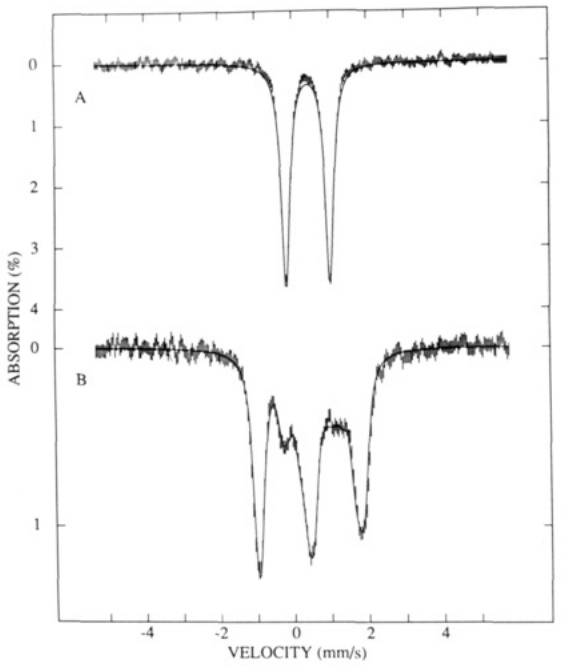

FIGURE 1: 4.2 K Mössbauer spectra of ^{57}Fe-enriched *E. coli* endonuclease III. (A) Spectrum recorded in zero field. (B) Spectrum recorded in an applied field of 6.0 T. The solid lines in (A) and (B) are a least-squares fit and a spectral simulation, respectively. The relevant parameters are $\Delta E_Q = +1.18$ mm/s, $\eta = 0.5$, $\delta = 0.44$ mm/s, and 0.27 mm/s line width.

diamagnet; i.e., the spectrum could be simulated by assuming that the iron nuclei experience only the applied field but no internal field. The solid line drawn through the data is a theoretical spectrum assuming four equivalent sites with $\Delta E_Q > 0$ and $\eta = 0.5$, where η is the asymmetry parameter of the electric field gradient tensor. It can be seen that the theoretical curve, simulated with the assumption of diamagnetism, fits the data very well.

The spectra of Figure 1, and spectra recorded with expanded velocity sweeps, showed no evidence for iron other than that associated with the 4Fe–4S cluster, and we conclude that impurity iron, if present, was less than 5% of the total Fe. After completing the Mössbauer studies, we used some of the sample to record an optical spectrum. This spectrum was identical with that reported by Asahara et al. (1989). Subsequently, we determined the Fe concentration of this sample, from which we obtained an extinction coefficient of 1.7×10^4 M^{-1} cm^{-1} at 410 nm.

We have also added a 5-fold excess of thymine glycol, an inhibitor of *N*-glycosylase activity, to ^{57}Fe-enriched endonuclease III and then recorded a Mössbauer spectrum. The spectrum was identical with that obtained for the native enzyme. However, we have not yet optimized the conditions for inhibitor studies, and this result, therefore, should be viewed with some caution.

EPR Studies. Oxidation of many protein-bound $[4Fe–4S]^{2+}$ clusters with ferricyanide causes the loss of one iron from the cluster, producing a $[3Fe–4S]^{1+}$ cluster (Beinert & Thomson, 1983). The latter typically exhibit EPR signals with *g* values near 2.01. An EPR spectrum of ferricyanide-oxidized endonuclease III, recorded at 10 K, is shown in Figure 2A. The spectrum is remarkably similar to that of oxidized beef liver cytoplasmic aconitase (Beinert & Thomson, 1983). At 10 K, the signal showed no evidence for power saturation at least up to 10 mW; at 50 K, the signal broadened to undetectability. Oxidations with a 3-fold molar excess of ferricyanide typically yielded 0.10–0.15 spin per 23.5-kDa monomer; the sample of

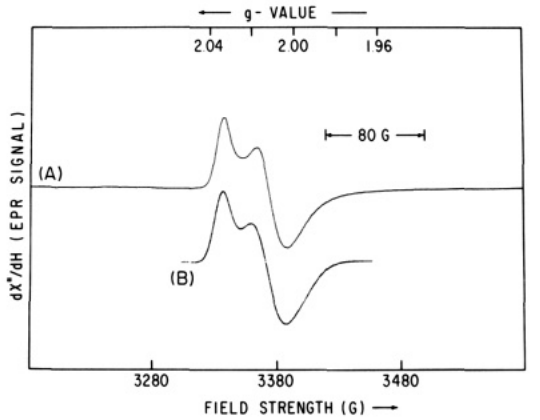

FIGURE 2: (A) EPR spectrum from endonuclease III, at a concentration of about 100 μM. The 0.2-mL sample was oxidized for about 10 min with a 3-fold molar excess of ferricyanide. Solvent was 0.1 M, pH 6.6 phosphate containing about 15% glycerol. Field modulation was 10 G ptp, and microwave power was 2.0 mW; field sweep of 400 G centered at 3380 G took 200 s with a 0.3-s experimental time constant. Temperature was 10 K. (B) Simulation of (A). *g* values were 2.030, 2.007, and 1.990, and the line widths corresponding to these *g* values were 8.0, 11.5, and 24.0 G, respectively.

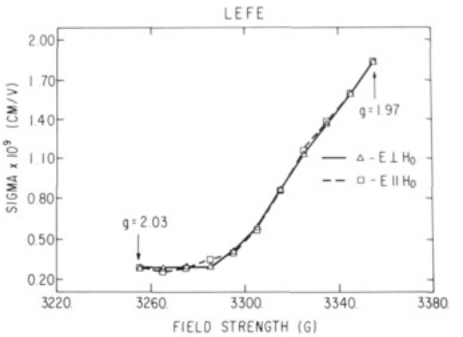

FIGURE 3: Magnetic field dependence of the linear electric field effect (LEFE). This figure shows the results of the LEFE experiment on ferricyanide-oxidized endonuclease III. The microwave frequency used was 9.209 GHz, the time between pulses was 750 ns, and the sample thickness was 0.2 cm. The parameter σ is proportional to the mean fractional shift in *g* per unit of applied electric field and was determined by using the procedure outlined by Mims and Peisach (1979). In the study shown, the electric field *E* was aligned either parallel to ($E_\parallel H_0$) or perpendicular to ($E_\perp H_0$) the magnetic field.

Figure 2A had about 0.25 spin per monomer. The spectrum shown in Figure 2B is a theoretical curve generated with the parameters quoted in the caption. (The EPR spectra of some samples of native enzyme exhibited a feeble $g = 2.01$ signal, accounting for less than 0.05 spin/cluster.)

Figure 3 shows the LEFE behavior of the ferricyanide-oxidized protein in which the LEFE parameter increased with increasing magnetic field both for $E_\parallel H_0$ and for $E_\perp H_0$; the shift parameter is very similar for both orientations of any magnetic field contained in the EPR absorption envelope. This behavior is remarkably similar to that observed for oxidized aconitase and other three-iron centers (Peisach et al., 1983; Ackrell et al., 1984). LEFE behavior identical with that shown in Figure 3, combined with the appearance of an EPR signal from a wide range of 3Fe–4S proteins obtained from 4Fe–4S proteins under oxidizing conditions, led Peisach et al. (1983) to conclude that such an LEFE pattern is a signature for oxidized 3Fe–4S centers. A comparison of the three-pulse ESEEM signals of protein in protonated solvent (Figure 4A) and deuterated solvent (Figure 4B) demonstrates the existence of exchangeable deuterons near the oxidized Fe–S center. The ESEEM "difference" spectrum obtained by FT of Figure 4C, which was obtained from the ratio of data in Figure 4B to those

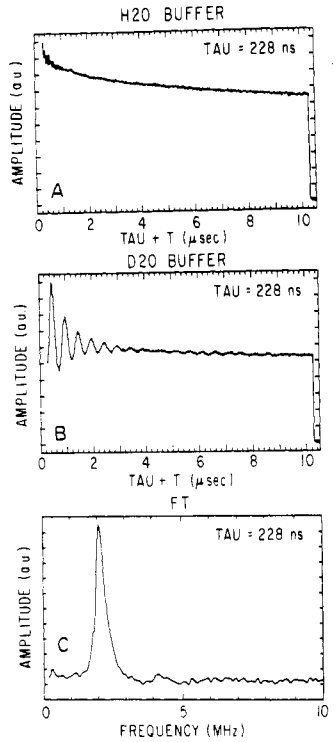

FIGURE 4: Three-pulse, stimulated echo ESEEM data collected for (A) a protonated sample and (B) a deuterated sample at $g = 2.01$. The microwave frequency was 8.7 GHz, pulse power 40 W, pulse width 20 ns, sample temperature 1.8 K, and pulse sequence repetition rate 100 Hz. The τ value used to collect these data was chosen to suppress matrix proton modulation while enhancing the contribution of magnetically coupled deuterons. (C) was obtained from the ratio of data of (B) to (A), which was then Fourier transformed to reveal a single peak near the deuteron NMR frequency of 2.01 MHz.

of Figure 4A, shows a single resonance at the deuteron NMR frequency. Shallow, low-frequency modulations were observed for samples suspended in aqueous buffer, but these components were not of sufficient intensity to be clearly resolved by Fourier transformation.

Upon photoreduction of an anaerobic sample of endonuclease III for 1.5 min, maximum bleaching of the 410-nm band was observed, suggesting that the 4Fe–4S cluster had been fully reduced. EPR of this sample shows a spectrum with g values at $g = 2.04$, 1.92, and 1.88 (Figure 5). Double integration yielded a spin concentration of 0.1–0.15 spin/4Fe cluster. In the presence of 10 mM thymine glycol, almost no bleaching of the 410-nm band was observed after 3 min of photoreduction. In addition, no EPR signals were observed. As a control, the photoreduction of aconitase was not affected by 10 mM thymine glycol. An oxidation of either photoreduced endonuclease III or aconitase brought the intensity of the 400–410-nm band to 80–90% of its original absorbance. These observations suggest that the presence of the inhibitor prevents the reduction of the cluster. The sample used exhibited originally a weak $g = 2.01$ signal. Interestingly, the 3Fe–4S cluster accounting for this weak signal was reduced in the presence of thymine glycol, as indicated by the disappearance of its $g = 2.01$ signal.

Discussion

According to chemical analyses, endonuclease III contains iron and sulfide in roughly stoichiometric proportions. The quadrupole and isomer shift parameters determined by Mössbauer spectroscopy of endonuclease III were typical of 4Fe–4S clusters in the 2+ core oxidation state (Münck & Kent, 1986). [Clusters with 2Fe–2S cores tyically have ΔE_Q

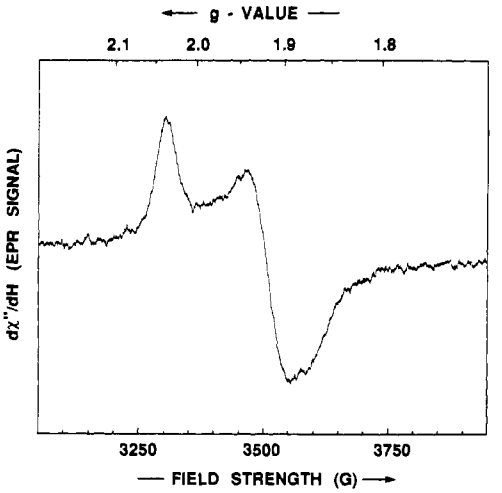

FIGURE 5: EPR spectrum of photoreduced endonuclease III at a concentration of 100 μM. Experimental conditions for obtaining the EPR spectrum were a temperature of 10 K, 1-mW microwave power, 8-G modulation amplitude, 9.419-GHz microwave frequency, 5 G/s sweep rate, and 0.08-s time constant.

= 0.4–0.8 mm/s and δ = 0.25–0.30 mm/s and thus have distinctly different parameters than those observed here (Münck & Kent, 1986).] In the 2+ state, such 4Fe–4S clusters exhibit pronounced valence delocalization, yielding equivalent Fe sites at the formal oxidation level $Fe^{2.5+}$ (Münck & Kent, 1986). All $[4Fe–4S]^{2+}$ cubanes studied thus far have a diamagnetic electronic ground state (Münck & Kent, 1986). Thus, the Mössbauer studies show unambiguously that the protein contains an iron–sulfur cluster with 4Fe–4S core stoichiometry. In the native enzyme, the cluster occurs in the diamagnetic 2+ core oxidation state which is the same state as observed for active aconitase (Kent et al., 1982, 1985) and glutamine phosphoribosylpyrophosphate amidotransferase (Averill et al., 1980; Vollmer et al., 1983). The Mössbauer spectrum is quite similar to that of the amidotransferase (Averill et al., 1980); thus, the clusters of both proteins have sharp lines and essentially temperature-independent quadrupole splittings. This is in contrast to aconitase (Kent et al., 1985) and other proteins with 4Fe–4S clusters which have inequivalent iron sites and pronounced temperature-dependent ΔE_Q values (Kent et al., 1985). The absorption lines of the observed quadrupole doublet are very sharp, indicating that the four iron subsites of the cluster reside in very similar environments. Although the electronic properties of 4Fe–4S clusters are dominated by the core structure of the cluster, the pronounced equivalence of the iron sites of endonuclease III suggests a homogeneous ligand structure; i.e., we suspect that each iron is coordinated to a cysteine residue.

The presence of an Fe–S cluster in endonuclease III is also supported by the EPR studies. Oxidation with ferricyanide yields a species with $g = 2.01$. Such signals are characteristic of oxidized 3Fe–4S clusters which result from oxidative removal of one iron from a 4Fe–4S cubane. Lack of deep ^{14}N features in the Fourier-transformed spin-echo pattern suggests lack of nitrogenous ligands, at least in the $[3Fe–4S]^{1+}$ oxidized form. The sensitivity to photoreduction of this oxidized 3Fe–4S endonuclease III in the presence of thymine glycol, combined with accessibility of exchangeable water to the Fe–S center, may suggest an altered conformation due to loss of one Fe.

The experiments indicate that with this Fe–S protein the $[4Fe–4S]^{2+}$ and $[4Fe–4S]^{1+}$ states are accessible but not the $[4Fe–4S]^{3+}$ state since the $[3Fe–4S]^{1+}$ state results on oxidation. Upon photoreduction, the $[4Fe–4S]^{1+}$ state is attained.

The g values of the reduced form are typical for the $S = {}^1/_2$ form of a reduced $[4Fe-4S]^{1+}$ cluster (Cammack et al., 1985). Since the bleaching of the optical spectrum of the sample suggested full reduction, it is possible that the majority of the cluster is in a spin state with $S \geq {}^3/_2$. It has been shown recently that the $[4Fe-4S]^{1+}$ clusters in proteins (Lindahl et al., 1985; Auric et al., 1987) and synthetic analogues (Carney et al., 1988) can exist in a spin mixture of $S = {}^1/_2$, $S = {}^3/_2$ (and perhaps $S = {}^5/_2$) states. The $S = {}^3/_2$ form yields generally broad bands of low signal amplitude between $g = 6$ and 4. The sample used for the photoreduction was too dilute to permit observation of such signals. The difficulties we encountered in oxidizing or reducing the Fe–S cluster of endonuclease III are similar to those reported for amidotransferase (Vollmer et al., 1983).

A number of Fe–S proteins have been sequenced, and it is common to find cysteine-containing runs as reported in the previous sequence paper on endonuclease III (Asahara et al., 1989), e.g., Cys-X-Y-Cys, where the cysteine is bound to the iron. Fe–S proteins have characteristic highly conserved sequences in the vicinity of the cluster (Fukuyama et al., 1988). $[2Fe-2S]^{2-}$ proteins have the Cys-X-Y-Cys sequence, followed by a third cysteine after a short segment of amino acid residues (usually four); the fourth cysteine in the cluster's set of ligands is usually far removed in the sequence. 4Fe–4S clusters are often associated with Cys-X-Y-Cys-X-Y-Cys sequences (Fukuyama et al., 1988). The binding domain for the 3Fe–4S cluster in the 7Fe ferredoxins involves three cysteines each separated by seven or more amino acids (Stout et al., 1988). However, examples of other sequences associated with all three types of cluster are known. Sequence information alone is therefore not sufficient to predict the occurrence of a cluster or to determine its type in the absence of other data.

The presence of a 4Fe–4S cluster in endonuclease III leads to speculation as to what role it plays in the enzyme. Possible functions include a role in the catalytic mechanism such as is seen in aconitase where the 4Fe–4S cluster binds substrates, or it may have a regulatory or structural function as has been proposed for the cluster of amidotransferase. With the advent of cloning and overexpression of this enzyme (Asahara et al., 1989), there is sufficient material for spectroscopic and analytical studies needed to elucidate the role of the 4Fe–4S cluster in endonuclease III. Such studies are in progress.

Acknowledgments

We are particularly grateful to Dr. Katherine Gibson, who first pointed out to us that endonuclease III might be an Fe–S protein. We thank Linda P. Welch for preparation of the manuscript.

Registry No. *Escherichia coli* endonuclease III, 60184-90-9.

References

Ackrell, B. A. C., Kearney, E. B., Mims, W. B., Peisach, J., & Beinert, H. (1984) *J. Biol. Chem. 259*, 4015–4018.

Asahara, H., Wistort, P. M., Bank, J. F., Bakerian, R. H., & Cunningham, R. P. (1989) *Biochemistry* (preceding paper in this issue).

Auric, P., Gaillard, J., Meyer, J., & Moulis, J.-M. (1987) *Biochem. J. 242*, 525–530.

Averill, B. A., Dwivedi, A., Debrunner, P., Vollmer, S. J., Wong, J. Y., & Switzer, R. L. (1980) *J. Biol. Chem. 255*, 6007–6010.

Bailly, V., & Verly, W. G. (1987) *Biochem. J. 242*, 565–572.

Beinert, H. (1983) *Anal. Biochem. 131*, 373–378.

Beinert, H., & Thomson, A. J. (1983) *Arch. Biochem. Biophys. 222*, 333–361.

Beinert, H., Emptage, M. H., Dreyer, J.-L., Scott, R. A., Hahn, J. E., Hodgson, K. O., & Thomson, A. J. (1983) *Proc. Natl. Acad. Sci. U.S.A. 80*, 393–396.

Breimer, L. H., & Lindahl, T. (1980) *Nucleic Acids Res. 8*, 6199–6211.

Breimer, L. H., & Lindahl, T. (1984) *J. Biol. Chem. 259*, 5543–5548.

Breimer, L. H., & Lindahl, T. (1985) *Biochemistry 24*, 4018–4022.

Cammack, R., Patil, D. S., & Fernandez, V. M. (1985) *Biochem. Soc. Trans. 13*, 572–578.

Carney, M. J., Papaefthymiou, G. C., Spartolian, K., Frankel, R. B., & Holm, R. H. (1988) *J. Am. Chem. Soc. 110*, 6084–6095.

Demple, B., & Linn, S. (1980) *Nature (London) 287*, 203–208.

Doetsch, P. W., Helland, D. E., & Haseltine, W. A. (1986) *Biochemistry 25*, 2212–2220.

Doetsch, P. W., Henner, D. E., Cunningham, R. P., Toney, J. H., & Helland, D. E. (1987) *Mol. Cell. Biol. 7*, 26–32.

Emptage, M. H. (1988) *ACS Symp. Ser. No. 372*, 343–371.

Fogo, J. K., & Popowsky, M. (1949) *Anal. Chem. 21*, 732–737.

Fukuyama, K., Nagahara, Y., Tsukihara, T., Katsube, Y., Hase, T., & Matsubara, Y. (1988) *J. Mol. Biol. 199*, 183–193.

Helland, D. E., Doetsch, P. W., & Haseltine, W. A. (1986) *Mol. Cell. Biol. 6*, 1983–1990.

Katcher, H. L., & Wallace, S. S. (1983) *Biochemistry 22*, 4071–4081.

Kennedy, M. C., Kent, T. A., Emptage, M., Merkle, H., Beinert, H., & Münck, E. (1984) *J. Biol. Chem. 259*, 14463–14471.

Kennedy, M. C., Werst, M., Telser, J., Emptage, M. H., Beinert, H., & Hoffman, B. M. (1987) *Proc. Natl. Acad. Sci. U.S.A. 84*, 8854–8858.

Kent, T. A., Dreyer, J.-L., Kennedy, M. C., Huynh, B. H., Emptage, M. H., Beinert, H., & Münck, E. (1982) *Proc. Natl. Acad. Sci. U.S.A. 79*, 1096–1100.

Kent, T. A., Emptage, M. H., Merkle, H., Kennedy, M. C., Beinert, H., & Münck, E. (1985) *J. Biol. Chem. 260*, 6871–6881.

Kow, Y. W., & Wallace, S. S. (1987) *Biochemistry 26*, 8200–8206.

Kurtz, D. M., Holm, R. H., Ruzicka, F. J., Beinert, H., Coles, C. J., & Singer, T. P. (1979) *J. Biol. Chem. 254*, 4967–4969.

Lindahl, P. A., Day, E. P., Kent, T. A., Orme-Johnson, W. H., & Münck, E. (1985) *J. Biol. Chem. 260*, 11160–11173.

Massey, V., & Hemmerich, P. (1978) *Biochemistry 17*, 9–17.

McCracken, J., Peisach, J., & Dooly, D. M. (1987) *J. Am. Chem. Soc. 109*, 4064–4077.

Mims, W. B. (1974) *Rev. Sci. Instrum. 45*, 1583–1591.

Mims, W. B., & Peisach, J. (1979) in *Biological Applications of Magnetic Resonance* (Shulman, R. G., Ed.) pp 221–269, Academic Press, New York.

Münck, E., & Kent, T. A. (1986) *Hyperfine Interact. 27*, 161–172.

Peisach, J., Beinert, H., Emptage, M. H., Mims, W. B., Fee, J. A., Orme-Johnson, W. H., Rendina, A. R., & Orme-Johnson, N. R. (1983) *J. Biol. Chem. 258*, 13014–13016.
Salerno, J. C., & Ohnishi, T. (1980) *Biochem. J. 192*, 769–781.
Siegel, L. M., Murphy, M. J., & Kamin, H. (1973) *J. Biol. Chem. 248*, 251–264.
Stout, G. H., Turley, S., Sieker, L. C., & Jensen, L. H. (1988) *Proc. Natl. Acad. Sci. U.S.A. 85*, 1020–1022.
Telser, J., Emptage, M. H., Merkle, H., Kennedy, M. C., Beinert, H., & Hoffman, B. M. (1986) *J. Biol. Chem. 261*, 4840–4846.
Vollmer, S. J., Switzer, R. L., & Debrunner, P. G. (1983) *J. Biol. Chem. 258*, 14284–14293.
Weiss, R. B., & Duker, N. J. (1986) *Nucleic Acids Res. 14*, 6621–6631.
Weiss, R. B., & Duker, N. J. (1987) *Photochem. Photobiol. 45*, 763–768.

Specific Activation of Open Complex Formation at an *Escherichia coli* Promoter by Oligo(*N*-methylpyrrolecarboxamide)s: Effects of Peptide Length and Identification of DNA Target Sites†

Pamela A. Martello,‡ James P. Bruzik,‡ Pieter deHaseth,*,‡ R. Scott Youngquist,§ and Peter B. Dervan§

Department of Biochemistry, School of Medicine, Case Western Reserve University, Cleveland, Ohio 44106, and Division of Chemistry and Chemical Engineering, California Institute of Technology, Pasadena, California 91125

Received November 21, 1988; Revised Manuscript Received February 1, 1989

ABSTRACT: It has previously been shown that open complex formation at a promoter containing a block substitution of nonalternating A-T sequences in the spacer DNA separating the contacted −10 and −35 regions could be accelerated by distamycin. No stimulation was observed at a promoter with a substitution of alternating A-T base pairs in the same region or at the promoter with wild-type spacer. Here we compare the effect of distamycin [tris(*N*-methylpyrrolecarboxamide), formally a P3] with that of its extended homologues P4, P5, and P6. It is found that the stimulatory potential of these synthetic oligopeptides which bind in the minor groove of DNA ranks in the order P4 > (distamycin, P5) > P6. The interaction of these peptides with the three promoters was studied by monitoring the positions of the promoter DNA protected from MPE–Fe(II) cleavage in the presence of different concentrations of ligand. The results suggest that a higher affinity of oligopeptide for the spacer DNA than for the −10 and/or −35 region is a necessary, but not sufficient condition for stimulation. Different patterns of protected DNA regions are seen with each of the three promoters; with distamycin, P4, and P5, a unique arrangement of protected regions is observed for the variant containing nonalternating A-T base pairs in its spacer DNA. These data support the hypothesis that differences in the ways the minor-groove binders interact with each of the promoter variants account for the observed differential stimulation. We further postulate that it is a ligand-induced structural change in the nonalternating A-T DNA which is responsible for the activation of open complex formation at the promoter containing this substitution.

In the process of transcription initiation at a bacterial promoter, RNA polymerase interacts specifically with two highly conserved hexamers located at positions −10 and −35 relative to the start site of transcription (von Hippel et al., 1984; McClure, 1985). These sequences are separated by a spacer DNA (consensus length 17 base pairs), which is devoid of contacts with polymerase (Siebenlist et al., 1980; Auble et al., 1986) over a stretch of about 10 base pairs. We have constructed a collection of promoter variants bearing, in this region of the spacer, substitutions with nine base pairs of various sequences that have the ability to adopt conformations other than typical B-DNA. Using these variants, we have been able to demonstrate that the intrinsic structure of the spacer region can affect the interaction between RNA polymerase and promoter DNA (Auble et al., 1986). In subsequent studies, promoter variants S(TT), S(AT), and S(wt) (Figure 1) were exposed to sequence-specific DNA-binding ligands, in the hope of targeting them to the spacer regions and thus extrinsically altering the structure of these promoters. The addition of the tripeptide distamycin to S(TT) resulted in a specific increase in functional complex formation at this promoter (Bruzik et al., 1987).

Distamycin, like the related antitumor antibiotic netropsin, binds along the minor groove of DNA in A,T-rich regions of DNA through hydrogen bonds and hydrophobic interactions (Zimmer & Wahnert, 1986; Kopka et al., 1985; Coll et al., 1987). The structures of distamycin and the synthetic homologues (P4–P6) studied in this paper are shown in Figure 2. The synthetic peptides differ from each other in the number of *N*-methylpyrrolecarboxamide residues. Like distamycin, P4, P5, and P6 bind preferentially to A,T-rich regions of DNA (Schultz & Dervan, 1983; Youngquist & Dervan, 1985). The binding site size on the DNA increases with increasing number

† P.B.D. and P.d.H. are grateful to the National Institutes of Health for research support (GM-27681 and GM-31808, respectively).
* Address correspondence to this author.
‡ Case Western Reserve University.
§ California Institute of Technology.

0006-2960/89/0428-4455$01.50/0